

Fuzzy Modulated Model Predictive Control of a PV grid-tied Quasi-Z-Source System

Salah Anis Krim¹, Abdelouahad May², Fateh Krim³

^{1,2,3}Department of electronics, University of Setif-1, Setif, Algeria

Corresponding author: Fateh Krim (krim_f@iceee.org).

Abstract

This paper investigates the design of a novel photovoltaic (PV) grid-tied quasi-Z-source inverter (qZSI) controller, combining the Modulated Model Predictive Control (M²PC) and Fuzzy Logic Control (FLC) techniques. The performance is compared to a Conventional M²PC (CM²PC) controller. To extract the maximum PV power a straightforward current-based Perturb and Observe Maximum Power Point Tracking (P&O-MPPT) algorithm is employed to generate the reference current for the FL controller. The suggested controller exhibits a high power efficiency, as well as rapid and effective tracking dynamics. In addition, it can autonomously inject current into the grid with a power factor close to unity. Through comprehensive simulation and comparative analysis, the high performance of the proposed controller is demonstrated, in terms of efficiency, accuracy, speed, power quality and robustness.

Keywords

qZSI, Photovoltaic, Power quality, M²PC, FLC.

1. Introduction

Renewable energy, including solar power, is crucial today due to climate change and resource depletion. Solar energy is clean, abundant, and reduces emissions. Its decentralization empowers communities and enhances energy security. Advancements in technology make solar more efficient and affordable [1-3].

Embracing solar power has created a surge in research and development efforts in the field of power electronics and renewable energy systems. As the demand for more efficient, reliable, and environmentally friendly power conversion solutions grows, inverters have emerged as critical components in various applications, ranging from renewable energy integration to motor drives and industrial power supplies [4, 5]. In this context, one noteworthy and innovative inverter topology that has garnered significant attention is the qZSI. The qZSI is a variation of the traditional Z-Source Inverter (ZSI), characterized by its unique impedance network. This specialized inverter has demonstrated promising capabilities to enhance power conversion performance, offer better efficiency, and address certain operational challenges [6-9].

Control methods in the qZSI have been the subject of extensive research and development, aiming to enhance their efficiency and performance across various applications [10]. Among the conventional control techniques commonly used with the qZSI are Proportional-Integral-Derivative (PID) [11], Pulse Width Modulation (PWM) [12], Space Vector Modulation (SVM) [13, 14], and Model Predictive Control (MPC) [15, 16]. These innovative control techniques have been introduced to improve the performance and efficiency of qZSI power systems. To enhance dynamic responses beyond the capabilities of PI-based control, several advanced control methodologies have been developed. These include neural network control [17], non-linear FLC [18], MPC [19-23], and sliding mode control (SMC) [10, 24-26]. The challenge with these proposed techniques is adjusting this paper introduces a novel approach that combines FLC for managing the duty-cycle of the qZSI with M²PC to the CM²PC concerning its ability to control the qZSI duty-cycle. This research aims to demonstrate the superiority of the proposed approach in managing the qZSI system. The evaluation criteria include factors such as current oscillations, control speed, and quality of grid-current.

2. Quasi-Z source inverter structure

2.1. Topology

Erreur ! Source du renvoi introuvable. illustrates a PV system consisting of solar panels and a qZSI converter connected to the grid. A qZSI is a type of power electronic converter that plays a crucial role in energy conversion and control systems. This innovative inverter topology is designed to overcome the limitations of traditional voltage-source inverters (VSI) and current-source inverters (CSI). The qZSI operates by utilizing an impedance network, typically implemented using a coupled inductor and a capacitor, to provide a unique feature of voltage buck-boost capability. The qZSI consists of several key components that work together to enable its functionality. These components include two capacitors C_2 and C_1 , and two inductors L_2 and L_1 , where $L_2=L_1=L$, $C_2=C_1=C$.

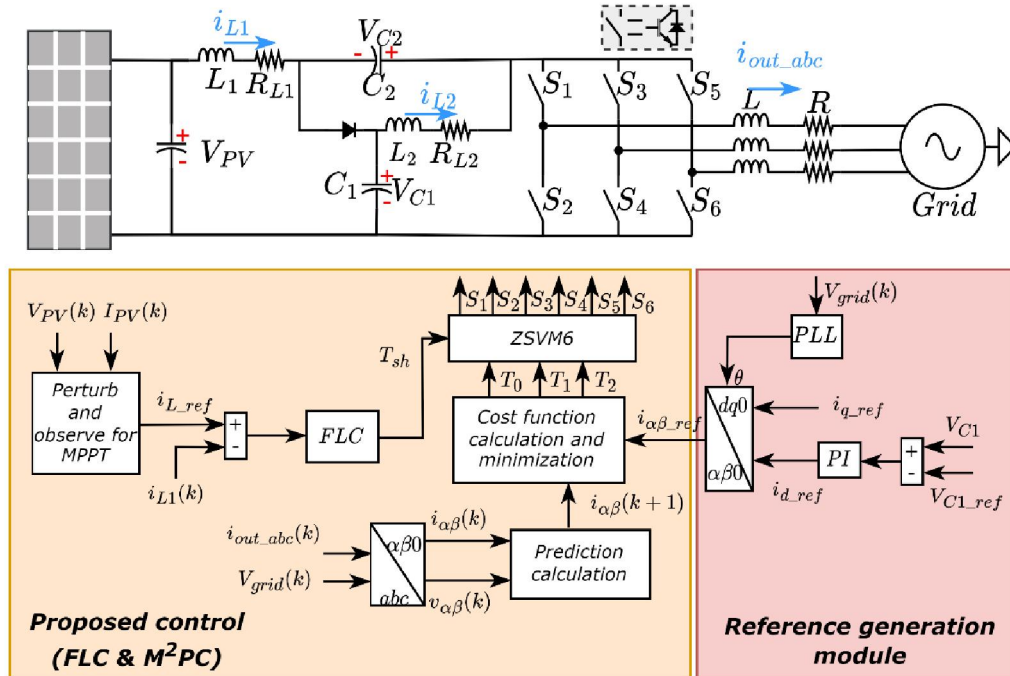


Fig.1. Proposed control structure for PV grid-tied qZSI

2.2. Operation principle

The shoot-through state (ST) and the non-shoot-through or active state (NST) are the two operating modes of the qZSI, as illustrated in **Erreur ! Source du renvoi introuvable.**. In active mode, the inverter works similarly to a VSI, as shown in Fig. 3 (a). In ST mode, Fig. 3 (b), the two switches within the same circuit leg are turned on simultaneously.

The current of the inductor L_1 is computed as follows based on the analogous circuit in the NST:

$$L \frac{di_{L1}}{dt} = V_{PV} - v_{C1} \quad (1)$$

where i_{L1} , v_{C1} , and V_{PV} stand for the inductor L_1 current, capacitor C_1 voltage, input voltage and, respectively. L represents the inductor's inductance.

$$L \frac{di_{L1}}{dt} = v_{C1} \quad (2)$$

By the grid-tied qZSI's state-space average model,

$$V_{dc} = \frac{1}{1-2D} V_{PV} \quad (1)$$

D stands for the ST duty-cycle.

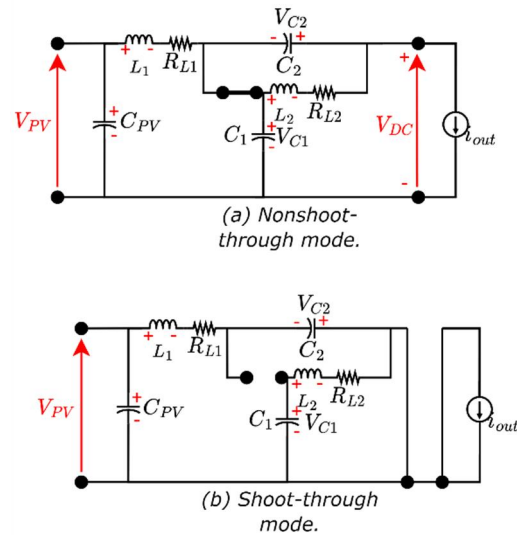


Fig. 2 qZSI operating modes a)NST b)ST

3. Proposed controller

Considering the distinctive characteristics of qZSI, an appropriate control technique must be implemented to ensure maximum utilization of these features. This paper proposes M²PC with an FLC of the ST. This combination of controls has been proposed to enhance the control quality of the direct current (DC) and reduce the harmonic distortion of the injected current into the grid. The suggested general controller concept is shown in Fig. 1.

3.1. Modulated model predictive control

M²PC integrates an appropriate modulation scheme minimizing the Cost Function (CF) within the MPC algorithm. In this study, a modulation scheme designed explicitly for qZSI control is implemented within the framework of M²PC with SVM for the qZSI, called the ZSVM6. The ZSVM6 controller concept is shown in **Erreur ! Source du renvoi introuvable.** (a). To achieve the concept of ZSVM6, the firing times were derived by proposing an FLC, as explained in the next section. In this section, we present the method of extracting traditional time intervals for SVM by controlling the output current of the converter with an M²PC.

The mathematical model utilized in this study employs the inverter's current output voltage vector (V) to inject power into the grid voltage $V_{grid_\alpha\beta}$ through an RL filter, resulting in the predictive equation for the output current. The continuous-time equation for the inverter grid interface is given by Eq (4). To make the computation feasible, this equation is then discretized using the forward Euler method, as provided by Eq (5). To further facilitate the computation process, each three-phase parameter is defined within a complex frame of reference represented by $(\alpha\beta)$. This approach effectively reduces the number of equations from three to one complex equation, significantly reducing the critical computation time for algorithms such as MPC.

$$V = Ri + L \frac{di}{dt} V_{grid_ \alpha\beta} \quad (4)$$

$$i_{\alpha\beta}(k+1) = i_{\alpha\beta}(k) \left[1 - \frac{R}{L} T_s \right] + \frac{T_s}{L} [V(k) - V_{grid_ \alpha\beta}(k)] \quad (5)$$

A CF is formulated to achieve the control objective, which incorporates the output current of the qZSI.

$$J = \| i_{\alpha\beta}(k+1) - i_{\alpha\beta}(k+1)^* \| \quad (2)$$

$i_{\alpha\beta}(k+1)$ and $i_{\alpha\beta}(k+1)^*$ stands for the output and reference current of the qZSI.

The CF is assessed for every prediction in M²PC, taking into account the ST and the two optimal vectors, to determine the duty-cycles. Three dues, J_1 , J_2 , and J_0 , are the outcome of this examination, where T_s stands for the sampling time. The following defines the corresponding duty-cycles:

$$\begin{cases} d_1 = T_S J_2 J_0 / (J_2 J_0 + J_1 J_0 + J_2 J_1) \\ d_2 = T_S J_1 J_0 / (J_2 J_0 + J_1 J_0 + J_2 J_1) \\ d_0 = T_S J_2 J_1 / (J_2 J_0 + J_1 J_0 + J_2 J_1) \end{cases} \quad (3)$$

where $J_1, J_2,$ and J_0 are the CF of vectors $(U_0, U_1$ and $U_2)$.

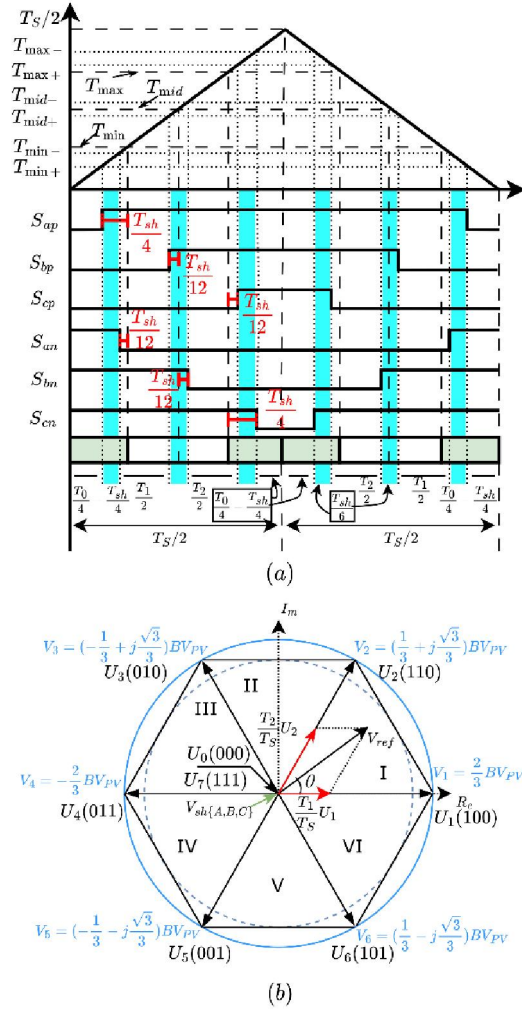


Fig. 3. (a) ZSVM6, (b) Switching states of the qZSI.

3.2. Fuzzy control of duty ratio

In this work, a new strategy for controlling the shoot-through time of qZSI has been developed using FLC, and this is without the need for a detailed mathematical model of the system. Fuzzification, a fuzzy rule base, and defuzzification are the three components that make up the fuzzy controller.

FLC has emerged as one of the best practical applications of fuzzy sets. The use of linguistic factors as opposed to numerical factors is one of its main features [28, 29]. The FLC approach is based on quality control regulations and depends on the human ability to understand the behavior of the system. This approach allows for a more intuitive and human-like control strategy, making it particularly suitable for systems with complex dynamics or uncertain environments.

The physical variables input's translation into fuzzy sets is possible through fuzzification. The variation of the error " ΔE " and the error " E " are our two inputs in this instance, and they are defined as follows:

$$E = \dot{i}_{L_ref}(n) - \dot{i}_L(n) \quad (4)$$

$$\Delta E = E(n) - E(n-1) \quad (5)$$

In the elicitation step, logical connections are established between the inputs and the output, represented by their respective membership functions as depicted in Fig. 4. These membership functions are utilized to determine the inference rules. Subsequently, a table of inference rules is constructed.

lists the 25 rules that make up the fuzzy D .

Table 1. Fuzzy Rule Base.

CE/E	NB	NS	Z	PS	PB
NB	Z	NM	NB	PS	PB
NS	NS	NS	NM	PS	PM
Z	NB	NS	Z	PS	PB
PS	NM	NS	PM	PS	PS
PB	NB	NS	PB	PM	Z

4. Simulation results

The proposed control technique for the studied system has been validated and compared with CM²PC based on the PI controller through computer simulation using “Simpower Systems” in MATLAB/Simulink®. Table1 presents the main system parameters. The system is analyzed separately to monitor the MPP while also independently managing the active power injection into the grid and observing the dynamic behavior of the controlled parameters.

Table1. Simulation parameters.

Parameters	Values
(P_{MPP}) STC Power	2519W
(I_{MP}) Current	24.90A
(V_{MP}) Voltage	101.16V
(V_s) AC Grid Voltage(RMS)	60V
(f) Grid Frequency	50Hz
$(C_1 \& C_2)$ qZS Capacitors	4700 μ F
(l) Line Inductor	10mH
(r) Parasitic Resistor	0.1 Ω
$(L_1 \& L_2)$ qZS Inductors	5mH
(f_s) Sampling Frequency	20kHz

The simulation results for the PV-side and AC-side steady-state operations are displayed in Fig.1 and Fig.2. In Fig.1, we observe the accuracy and speed at which the voltage V_{MP} and current I_{MP} reach their peak values, consequently achieving the maximum power output of PV panels P_{MPP} with remarkable quality and efficiency. As for Fig.2 (a), (b), and (c), they depict the steady-state behavior of capacitor C_2 voltage, DC voltage, and grid current, respectively. The pulsating DC-link indicates the boosting operation, with the system smoothly adhering to the given instructions and exhibiting no abrupt voltage spikes in the DC-Link. This guarantees the dynamic performance of the system and adheres to the current limits of the system.

In Fig.3, and Fig.4, we can observe the response of the proposed system and CM²PC when exposed to a sudden shift in solar radiation levels, transitioning from 800 W/m² to 1000 W/m² and then to 800 W/m². This rapid change in radiation induces a swift system reaction with minimal overshooting. As depicted in Fig.3 (a), and Fig.4 (a), current L_1 , and PV voltage achieve a stable state within just 50 ms, and the maximum change of current L_1 , and PV voltage is $\Delta I=2.5A$ and $\Delta V=2V$, respectively. As for the CM²PC, the current L_1 , and PV voltage reach a steady state within 60 ms, and the maximum change in current, and PV voltage is $\Delta I = 6.1A$ and $\Delta V = 7V$, respectively. As illustrated in Fig.3 (b), and Fig.4 (b).

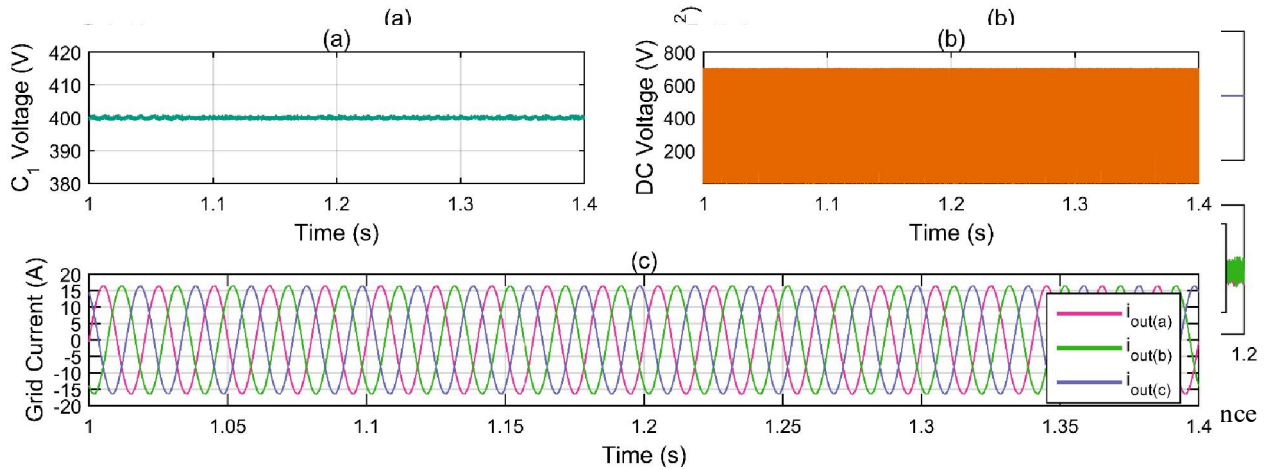


Fig.2. Results regarding the DC and AC-sides: (a) Capacitor C_2 voltage, (b) DC voltage, (c) Three-phase grid currents.

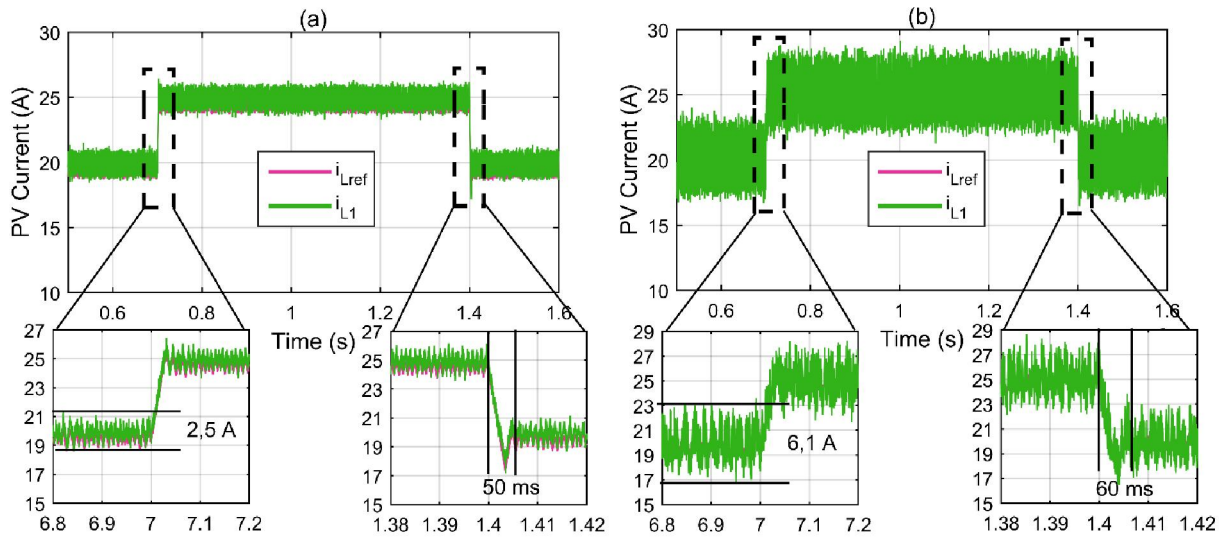


Fig.3. Inductance L_1 current results for the change in abrupt solar radiation: (a) proposed control, (b) CM²PC.

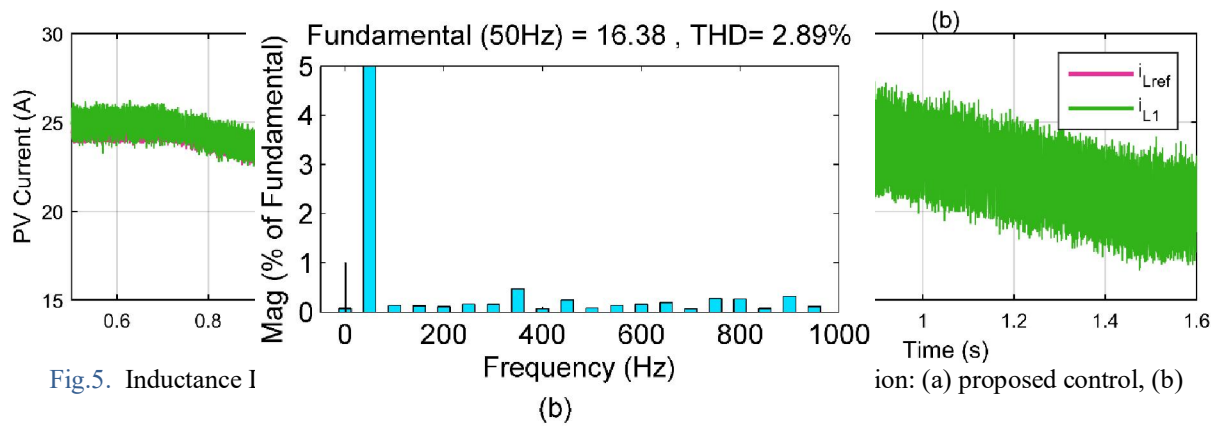
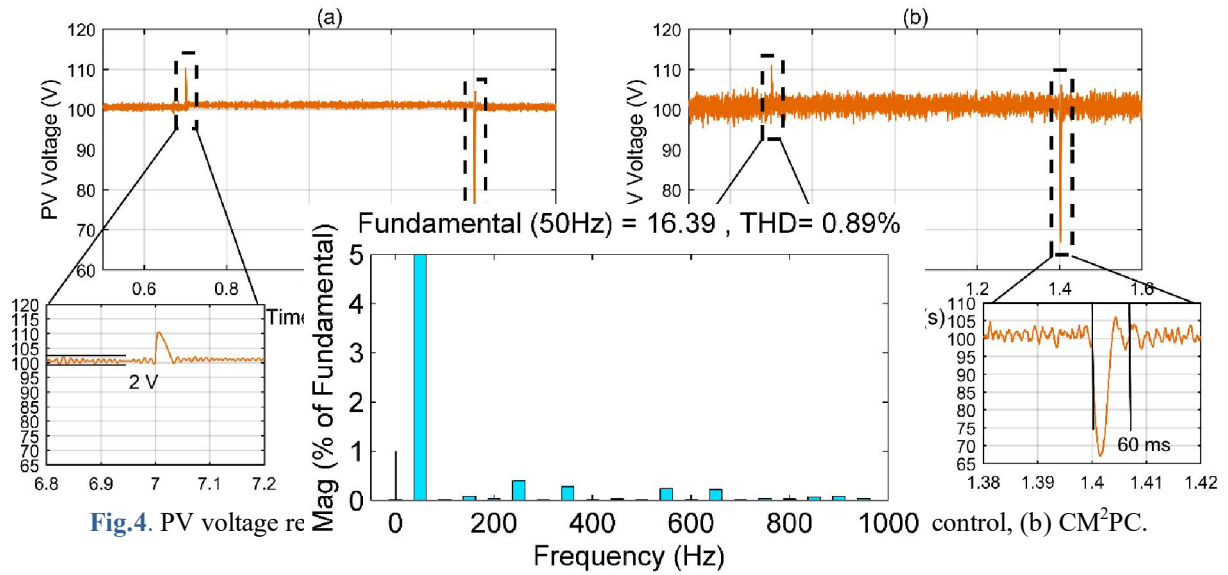


Fig. 9. Spectral analysis of the grid current: (a) proposed control, (b) CM²PC.

The proposed system has proven to excel in response speed, surpassing the CM²PC by 16.67%. One of the key strengths of the proposed system lies in its significant superiority over the CM²PC in terms of the maximum change in L_1 current and photovoltaic voltage. The percentage difference between them amounted to 59.01% and 71.43%, respectively, as shown in

Table 2. This advantage on the PV-side positively impacts the AC-side. As illustrated in Fig. , the comparison is conducted of the THD ratio of the proposed system's grid current and the CM²PC, where the difference between them is 69.21%.

Table 2. Comparative analysis of the suggested and CM²PC methods.

	Time to steady-state (T)		The maximum change (Δ)		THD %
	Current (ms)	Voltage (ms)	Current (A)	Voltage (V)	
CM ² PC	60	60	6.1	7	2.89
Proposed method	50	50	2.5	2	0.89
The percentage difference (%)	16.67	16.67	59.01	71.43	69.21

4. Conclusions

In this paper, a grid-connected qZSI control system based on a combination of M²PC and FLC is proposed and compared with a CM²PC. To achieve continuous operation of the PV system at its MPP, a straightforward current-based P&O-MPPT algorithm was employed to generate the reference current for the FL controller. The proposed system exhibited excellent capabilities in tracking and delivering maximum power from the PV source, characterized by rapid and efficient tracking dynamics. Moreover, it demonstrated the capability to independently inject current into the grid. The simulation and comparison results verified the strong performance of the implemented control techniques and the usefulness of the proposed system, showcasing its strong performance in regulating the grid-connected PV system.

References

- [1] A. May, F. Krim, H. Feroura, and A. Belaout, "Power Quality Enhancement of Grid-Tied 7L-PUC Inverter-Based PV System Using a Novel DC-Link Controller," *Arabian Journal for Science and Engineering*, pp. 1-15, 2023, doi: <https://doi.org/10.1007/s13369-023-08074-3>.
- [2] W. Rui, S. Qiuye, Z. Pinjia, G. Yonghao, Q. Dehao, and W. Peng, "Reduced-order transfer function model of the droop-controlled inverter via Jordan continued-fraction expansion," *IEEE Transactions on Energy Conversion*, vol. 35, no. 3, pp. 1585-1595, 2020, doi: <https://doi.org/10.1109/TEC.2020.2980033>.
- [3] D. Ma, K. Cheng, R. Wang, S. Lin, and X. Xie, "The decoupled active/reactive power predictive control of quasi-Z-source inverter for distributed generations," *International Journal of Control, Automation and Systems*, vol. 19, pp. 810-822, 2021, doi: <https://doi.org/10.1007/s12555-019-0698-9>.
- [4] S. Vadi, R. Bayindir, and E. Hossain, "A review of control methods on suppression of 2 ω ripple for single-phase quasi-Z-source inverter," *IEEE Access*, vol. 8, pp. 42055-42070, 2020, doi: <https://doi.org/10.1109/ACCESS.2020.2976581>.
- [5] S. M. Dabour, N. El-hendawy, A. A. Aboushady, M. E. Farrag, and E. M. Rashad, "A Comprehensive Review on Common-Mode Voltage of Three-Phase Quasi-Z Source Inverters for Photovoltaic Applications," *Energies*, vol. 16, no. 1, p. 269, 2022, doi: <https://doi.org/10.3390/en16010269>.
- [6] Y. Liu, B. Ge, H. Abu-Rub, and F. Z. Peng, "Overview of space vector modulations for three-phase Z-source/quasi-Z-source inverters," *IEEE Transactions on Power Electronics*, vol. 29, no. 4, pp. 2098-2108, 2013, doi: <https://doi.org/10.1109/TPEL.2013.2269539>.
- [7] M. A. V. Golande and A. Kinge, "Design and Analysis of Single Phase Modified Quasi-Z-Source Cascaded Hybrid Three Level Inverter," 2019.
- [8] M. R. Nayak, V. Tulasi, K. D. Teja, K. Koushic, and B. S. Naik, "Implementation of quasi Z-source inverter for renewable energy applications," *Materials Today: Proceedings*, vol. 80, pp. 2458-2463, 2023, doi: <https://doi.org/10.1016/j.matpr.2021.06.383>.
- [9] M. Bubalo, M. Bašić, D. Vukadinović, and I. Grgić, "Hybrid wind-solar power system with a battery-assisted quasi-Z-source inverter: Optimal power generation by deploying minimum sensors," *Energies*, vol. 16, no. 3, p. 1488, 2023, doi: <https://doi.org/10.3390/en16031488>.
- [10] J. M. Ahangarkolaei, M. Izadi, and T. Nouri, "Applying Sliding Mode Control to Suppress Double Frequency Voltage Ripples in Single-phase Quasi-Z-source Inverters," *CSEE Journal of Power and Energy Systems*, vol. 9, no. 2, pp. 671-681, 2023, doi: <https://doi.org/10.17775/CSEEJPES.2022.02860>.
- [11] B. Balaji, K. S. S. Krishnan, R. Revathy, and R. Preetha, "Fractional order PID controlled quasi Z-source inverter with front-line semiconductor material made of power electronics switches fed PMSM motor for EV applications," *Materials Today: Proceedings*, vol. 69, pp. 1322-1333, 2022, doi: <https://doi.org/10.1016/j.matpr.2022.08.464>.
- [12] K. Chitra, V. Kamatchikannan, K. Viji, and M. Lakshmanan, "Simple boost PWM controlled cascaded quasi Z-source inverter," *Materials Today: Proceedings*, vol. 45, pp. 3161-3169, 2021, doi: <https://doi.org/10.1016/j.matpr.2020.11.1028>.
- [13] C. Qin, C. Zhang, A. Chen, X. Xing, and G. Zhang, "A space vector modulation scheme of the quasi-Z-source three-level T-type inverter for common-mode voltage reduction," *IEEE Transactions on Industrial Electronics*, vol. 65, no. 10, pp. 8340-8350, 2018, doi: <https://doi.org/10.1109/TIE.2018.2798611>.
- [14] C. Qin, X. Xing, and Y. Jiang, "Hybrid space vector modulation scheme to reduce common-mode voltage magnitude and frequency in three-level quasi-Z-source inverter," *IEEE Journal of Emerging and Selected Topics in Power Electronics*, vol. 10, no. 6, pp. 6810-6821, 2021, doi: <https://doi.org/10.1109/JESTPE.2021.3137609>.
- [15] M. Mosa, H. Abu-Rub, and J. Rodriguez, "High performance predictive control applied to three phase grid connected Quasi-Z-Source Inverter," in *IECON 2013-39th Annual Conference of the IEEE Industrial Electronics Society*, 2013: IEEE, pp. 5812-5817, doi: <https://doi.org/10.1109/IECON.2013.6700087>.

- [16] A. Bakeer, M. A. Ismeil, and M. Orabi, "A powerful finite control set-model predictive control algorithm for quasi Z-source inverter," *IEEE Transactions on Industrial Informatics*, vol. 12, no. 4, pp. 1371-1379, 2016, doi: <https://doi.org/10.1109/TII.2016.2569527>.
- [17] V. Rajasegharan, L. Premalatha, and R. Rengaraj, "Modelling and controlling of PV connected quasi Z-source cascaded multilevel inverter system: An HACSNM based control approach," *Electric Power Systems Research*, vol. 162, pp. 10-22, 2018, doi: <https://doi.org/10.1016/j.epsr.2018.04.020>.
- [18] T. Hou, C.-Y. Zhang, and H.-X. Niu, "Quasi-Z source inverter control of PV grid-connected based on fuzzy PCI," *Journal of Electronic Science and Technology*, vol. 19, no. 3, p. 100021, 2021, doi: <https://doi.org/10.1016/j.jnlest.2020.100021>.
- [19] Y. Guo, H. Sun, Y. Zhang, Y. Liu, X. Li, and Y. Xue, "Duty-cycle predictive control of quasi-Z-source modular cascaded converter based photovoltaic power system," *IEEE Access*, vol. 8, pp. 172734-172746, 2020, doi: <https://doi.org/10.1109/ACCESS.2020.3024935>.
- [20] M. A. Ismeil, O. Abdel-Rahim, H. S. Hussein, and E. H. Abdelhameed, "Implementation of New Optimal Control Methodology of Quazi Z-Source Inverter Based on MPC," *IEEE Access*, 2023, doi: <https://doi.org/10.1109/ACCESS.2023.3283297>.
- [21] S. K. Gannamraju and R. Bhimasingu, "Sequential model predictive control of quasi Z-source inverter with fixed frequency operation," *International Transactions on Electrical Energy Systems*, vol. 31, no. 11, p. e13068, 2021, doi: <https://doi.org/10.1002/2050-7038.13068>.
- [22] Y. Xu, Y. He, H. Li, and H. Xiao, "Model predictive control using joint voltage vector for quasi-Z-source inverter with ability of suppressing current ripple," *IEEE Journal of Emerging and Selected Topics in Power Electronics*, vol. 10, no. 1, pp. 1108-1124, 2021, doi: <https://doi.org/10.1109/JESTPE.2021.3106048>.
- [23] L. Li, T. Yang, Y. Yuan, and Z. Cai, "A model predictive control strategy based on energy storage grid-connected quasi-z-source inverters," *IET Generation, Transmission & Distribution*, vol. 16, no. 17, pp. 3451-3461, 2022, doi: <https://doi.org/10.1049/gtd2.12534>.
- [24] X. Duan, L. Kang, H. Zhou, and Q. Liu, "Multivector model predictive power control with low computational burden for grid-tied quasi-Z-source inverter without weighting factors," *IEEE Transactions on Power Electronics*, vol. 37, no. 10, pp. 11739-11748, 2022, doi: <https://doi.org/10.1109/TPEL.2022.3174303>.
- [25] F. Peng, W. Xie, and J. Yan, "Compound robust control of permanent magnet synchronous motor based on quasi-Z source inverter," *IET Electric Power Applications*, 2023, doi: <https://doi.org/10.1049/elp2.12311>.
- [26] F. Bagheri, H. Komurcugil, O. Kukrer, N. Guler, and S. Bayhan, "Multi-input multi-output-based sliding-mode controller for single-phase quasi-Z-source inverters," *IEEE Transactions on Industrial Electronics*, vol. 67, no. 8, pp. 6439-6449, 2019, doi: <https://doi.org/10.1109/TIE.2019.2938494>.
- [27] Y. Li, S. Jiang, J. G. Cintron-Rivera, and F. Z. Peng, "Modeling and control of quasi-Z-source inverter for distributed generation applications," *IEEE Transactions on Industrial Electronics*, vol. 60, no. 4, pp. 1532-1541, 2012, doi: <https://doi.org/10.1109/TIE.2012.2213551>.
- [28] M. Ranjani and P. Murugesan, "Optimal fuzzy controller parameters using PSO for speed control of Quasi-Z Source DC/DC converter fed drive," *Applied soft computing*, vol. 27, pp. 332-356, 2015, doi: <https://doi.org/10.1016/j.asoc.2014.11.007>.
- [29] M. Zangeneh, E. Aghajari, and M. Forouzanfar, "A survey: Fuzzify parameters and membership function in electrical applications," *International Journal of Dynamics and Control*, vol. 8, pp. 1040-1051, 2020, doi: <https://doi.org/10.1007/s40435-020-00622-1>.